Acta Acustica united with Acustica
Vol. 105 (2019) 210 – 219

Technical and Applied Papers
DOI 10.3813/AAA.919301

Vortex Shedding and Modal Behavior of a Circular Cylinder Equipped with Flexible Flaps

Thomas F. Geyer[1], Laura Kamps[2], Ennes Sarradj[3], Christoph Brücker[4]
[1] Brandenburg University of Technology Cottbus - Senftenberg, 03046 Cottbus, Germany. thomas.geyer@b-tu.de
[2] Technical University Bergakademie Freiberg, 09599 Freiberg, Germany
[3] Technische Universität Berlin, 10587 Berlin, Germany
[4] City University London, London EC1V 0HB, United Kingdom

Summary
When a cylinder is subject to a flow, vortices will be shed that can lead to strong tonal noise. The modification of the cylinder with soft, flexible flaps made of silicone rubber has been shown to affect the vortex shedding cycle in a way that the Strouhal number associated with the vortex shedding suddenly jumps to a higher value at a certain Reynolds number. In the present study, the effect of the flexible flaps on the vortex shedding is further examined by subsequently reducing the number of flaps and additionally shortening their length. Acoustic measurements and camera recordings of the flap motion, performed in an aeroacoustic wind tunnel, suggest that the sudden jump of the Reynolds number is caused by the movement of the outer flaps. A comparison with the eigenfrequencies obtained from a numerical modal analysis of the different flap rings revealed that the cause of the Strouhal number jump is most likely a lock-in of the natural vortex shedding cycle with the next higher eigenfrequency of the outer flaps.

PACS no. 43.28.Ra

1. Introduction

Periodic vortex shedding from cylinders is a classical problem in aerodynamics and an important source of noise [1, 2]. The tones emitted by this dipole noise source are known as aeolian tones, a phenomenon first studied by Strouhal [3]. The control of vortex shedding by passive methods, such as surface protrusions, shrouds and near-wake stabilizers [4], rigid splitter plates [5, 6, 7], O-rings [8], grooves [9], tripping wire [10], riblets [11], dimples [12], spines [13] or porous material [14], is therefore of great interest for many potential applications.

In a water tunnel study by Kunze and Brücker [15] it has been shown that the presence of flexible flaps at the aft part of a circular cylinder strongly affects the vortex shedding behavior. This led to the fact that at a certain specific Reynolds number Re (based on cylinder diameter d) the Strouhal number Sr associated with vortex shedding quite suddenly increased from a value of about 0.23 to a value of 0.29. The result was a jump in the corresponding Reynolds-Strouhal number diagram (when instead of the cylinder diameter the streamwise length of the separation bubble was used to calculate the Strouhal number, no jump was visible). The reason for this effect was found to be a lock-in effect between the vortex shedding and the oscillation of the flexible flaps. Particle Image Velocimetry (PIV) measurements were conducted at Reynolds numbers of 5,000 to 31,000. The results showed that, due to the presence of the flaps, the vortices were not shed in a zig-zag like arrangement as in the classical von Kármán vortex street, but rather in-line in a row with the cylinder wake axis. Additionally, it was found that the size of the recirculation area behind the cylinders with flaps is notably smaller than the size of the recirculation area behind a reference cylinder.

A subsequent investigation [16], which was performed in an aeroacoustic wind tunnel, revealed that the change in vortex shedding also affected the emission of tonal noise, as the aeolian tones generated by a cylinder modified with eight flexible flaps were shifted to higher frequencies when above a certain Reynolds number. Besides the acoustic measurements, hot-wire anemometry measurements were performed, with the probe positioned one cylinder diameter downstream and one half diameter off center from the cylinders approximately at mid-span. Those measurements provided the power spectral density of the turbulent velocity fluctuations at this position, which also showed a peak due to the vortex shedding. For the cylinder with flaps, this measurement resulted in the same jump in the Reynolds-Strouhal number diagram, thus confirming the results from the acoustic measurements. It was concluded that the jump of the Strouhal number is caused by a lock-

Received 16 February 2018,
accepted 4 December 2018.

in between the vortex shedding peak and the resonances of the flap structures. Additionally, it was concluded that the outer flaps play a more important role than the inner flaps since they interact directly with the shear layer. Additionally, flow visualization experiments were performed. The results confirmed that the flexible flaps lead to a more slender separation bubble in the wake recirculation region compared to the reference cylinder.

It is interesting to note that an early experimental study has been performed by Grimminger [17] on cylinders modified with rigid "guide vanes", which, if properly designed, lead to a noticeable reduction in drag. However, although it is obvious that the cause of the drag reduction has to be an effect of the guide vanes on the flow pattern behind the cylinder, it was not observed if these guide vanes also affect the Strouhal number in a way similar to the observations made for the flexible flaps.

The effect found for the flexible flaps is also different from that observed for a single flexible splitter plate attached to a plain cylinder. In an experimental study by Shukla *et al.* [18] in a water tunnel at Reynolds numbers between 1,800 and 10,000 (based on cylinder diameter), two modes of periodic splitter plate motion were identified. Both modes featured a frequency close to the vortex shedding frequency of the cylinder, and thus no Strouhal number jump occurred. However, the Reynolds numbers were below the value were the jump was identified [15, 16] and the length of the flexible splitter plate was always greater than at least three cylinder diameters. In addition, the flexible splitter plates were constructed with spanwise stiffeners, and hence a three-dimensional deformation of the plates was prevented on purpose. Another experimental study on a flexible splitter plate in the wake of a cylinder was done by Teksin and Yayla [19], who performed PIV measurements in a water tunnel at a Reynolds number (based on cylinder diameter) of 2,500. They varied the length of the splitter plate (1.25 d, 2.25 d and 2.5 d, with d being the cylinder diameter) and found that it has a notable influence on the turbulence statistics in the wake. However, effects like the shedding of vortices in a row with the cylinder wake axis or a change of the size of the separation bubble, as observed for the cylinder with flexible flaps, were not visible.

The work presented here is a continuation of the study presented in [16]. Thereby, the focus is to further examine the fluid-structure-interaction and the assumed cause of the Strouhal number jump. To this end, acoustic measurements and flap motion measurements were performed on the original flap cylinder with eight flaps as used in [16] as well as on modified versions where, subsequently, flaps were cut off in order to determine their individual contribution to the observed vortex shedding behavior.

2. Materials and Methods

2.1. Cylinder Models

The flap cylinders consist of a core cylinder with a spanwise length l of 0.28 m and a diameter of 20 mm, on which

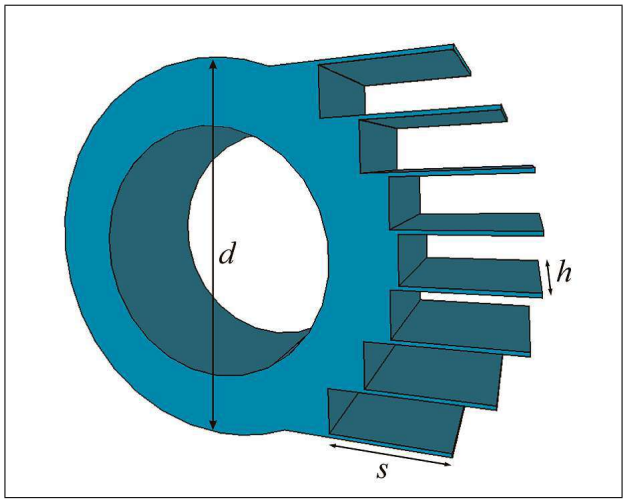

Figure 1. Schematic of the original flap ring with 8 flaps, as used in [16], showing outer diameter d as well as streamwise length s and width h of the flaps.

22 flap rings made of the silicone rubber Elastosil RT 601 were threaded. Thus, the flaps are not extended over the whole cylinder length, but divided into finite spanwise segments, which was done in order to disturb spanwise coherences. The thickness of the flap rings, and hence the width h of the flaps, was 12 mm. This value was chosen in order to obtain the same ratio of flap width to cylinder diameter $h/d = 0.4$ as in the original study by Kunze and Brücker [15].

The flap rings were cast using a casting mold consisting of metal plates with small gaps that will form the flaps. The original flap rings, as used in [16], contained eight flaps with a thickness of 0.3 mm. A schematic of this flap ring is shown in Figure 1. In the present study, measurements were also performed on modified flap rings, where a number of flaps was cut off from the original flap rings, resulting in cylinders with six, four and two flaps instead of eight. Figure 2 shows CAD models of the different flap rings used for this study. In most cases, the flaps had the original streamwise length s of 9 mm (Figure 2a through 2d). In the final experiments, the two remaining outer flaps were shortened to a length of $s = 4.5$ mm (Figure 2e).

Additionally, a plain cylinder was used as a reference in the experiments. All cylinder models had an outer diameter d of 30 mm, resulting in an aspect ratio l/d of 9.3. A photograph of the cylinder with six flaps is shown in Figure 3.

2.2. Modal Analysis

In order to enable a better understanding of the observed lock-in effect, the eigenmodes of the flap rings shown in Figure 2 were obtained numerically for frequencies up to 250 Hz using the block Lanczos algorithm implemented in Ansys (Academic Version R15.0). The flap rings were modelled as elastic, isotropic materials with a Young's modulus of 1.2 MPa, a density of 1080 kg/m^3 and a Poisson ratio of 0.495. The meshes for the Finite Element

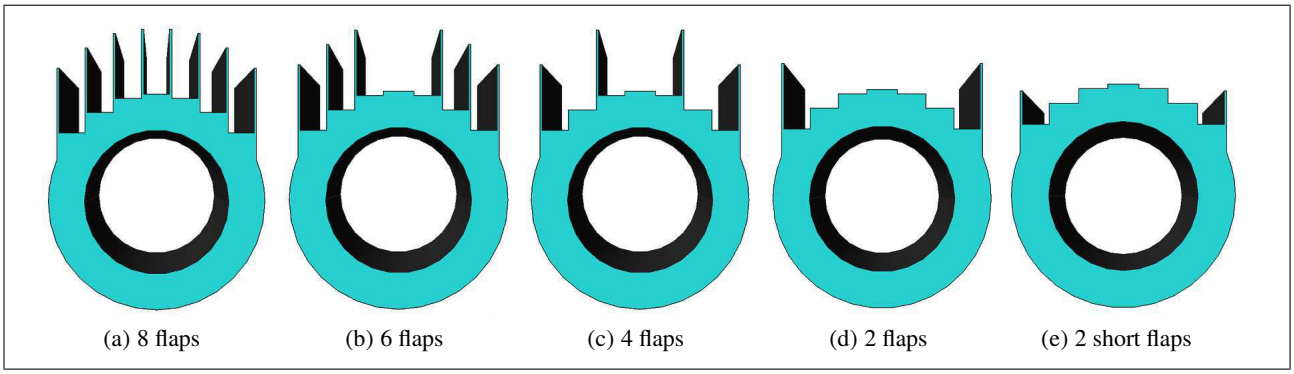

Figure 2. CAD models of the different flap ring versions used for the study.

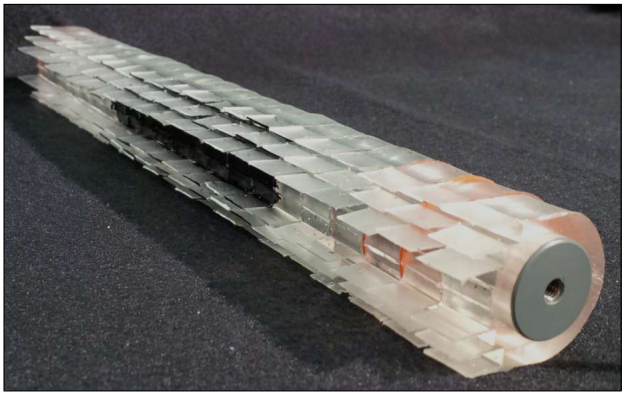

Figure 3. Photograph of the cylinder with six flaps (the flap rings at mid span are painted black to give a better contrast in the flap motion measurements).

Method (FEM) calculation consisted of 3-D 20-node solid tetrahedral elements with a maximum side length of 1 mm. For example, the mesh of the original cylinder with 8 flaps (see Figure 4) consisted of 6,840 elements. The influence of the mesh resolution on the resulting eigenfrequencies was tested for one of the models by using elements with a smaller maximum side length of 0.5 mm and 0.2 mm, thus increasing the element number from 6,540 to 49,008 and 730,500, respectively. Since the difference in the resulting eigenfrequencies was not significant (less than 2 %), a refinement of the mesh was not found necessary. As a boundary condition for the modal analysis it was defined that the inner surface of the flap ring (where the flap ring is in contact with the rigid core cylinder) will not be displaced.

It can be expected that the dimensions of the physical models of the flap rings may differ slightly from the CAD models due to the manufacturing process. This is especially true for the thickness of the flaps. To take a certain deviation of the nominal thickness of the flaps of 0.3 mm into account, eigenmodes and eigenfrequencies were additionally obtained for the case that the overall thickness of the flaps was increased by 5 % and 10 % to values of 0.315 mm and 0.33 mm as well as for the cases of a 5 % and 10 % decreased thickness of 0.285 mm and 0.27 mm. Of course, this rather simple procedure does not account for local deviations of the thickness of a single flap.

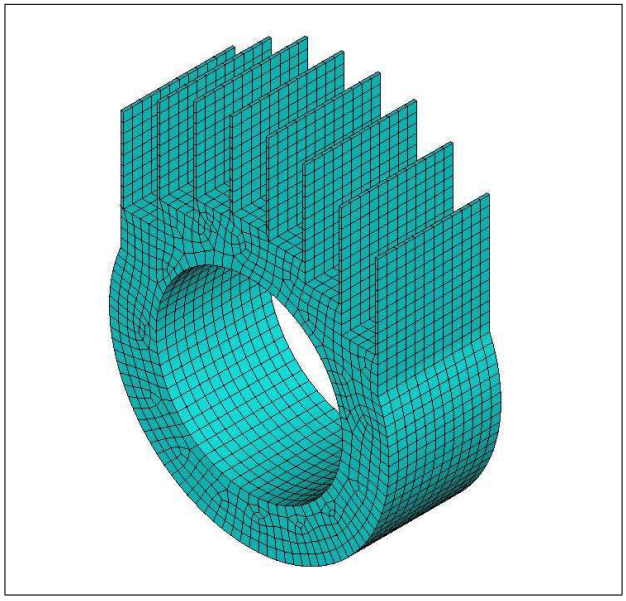

Figure 4. Mesh used for the modal analysis of the original flap ring with eight flaps.

2.3. Wind Tunnel

The experimental part of the study included acoustic measurements and measurements of the flap motion in the small aeroacoustic wind tunnel at Brandenburg University of Technology Cottbus – Senftenberg [20]. The test section used for the experiments has a rectangular cross-section of 0.28 m height × 0.23 m width. The top and bottom of this test section are made from acrylic glass, while the two side windows are covered with tensioned Kevlar, thus providing a two-dimensional flow, while at the same time enabling the use of an acoustic measurement technique positioned outside of the flow. Surrounding the test section is a cabin with absorbing side walls that lead to a nearly anechoic environment for frequencies above approximately 100 Hz.

In the experiments, the velocity was adjusted by setting the pressure in the wind tunnel settling chamber. The corresponding velocities were determined at the exit of the test section (with the reference cylinder in place) in a separate measurement, using a vane anemometer with an accuracy of ±0.2 m/s. The blockage due to the cylinders was

corrected using the simple approximative blockage correction method proposed by Barlow *et al.* [21].

Measurements were conducted at 13 subsonic flow speeds between 7 m/s and 17 m/s, leading to Reynolds numbers (based on outer cylinder diameter d) ranging from 14,600 to 34,000. In this range of flow speeds, the vortex shedding noise of the cylinders will be at frequencies below 200 Hz. In order to examine the reproducibility and to obtain a better statistical significance, each measurement was performed twice in individual runs.

2.4. Acoustic Measurements

The acoustic measurements were performed using two single one fourth inch free-field microphones positioned in a distance of 0.6 m on each side of the cylinder models. In the vertical direction, the microphones were pointed approximately at the mid-span location of the cylinders. Figure 5 shows a schematic and a photograph of the acoustic measurement setup.

The data were recorded with a sampling frequency of 51.2 kHz over a long time period of 90 s, using a 24 Bit National Instruments digital dynamic signal acquisition module (NI-USB 4431). Following the approach used in [16], the time signals from both microphones were added with a phase difference of 180°, assuming a theoretical dipole behavior of the cylinder generated noise. The data were then transformed in the frequency domain according to Welch's method [22] using a Fast Fourier Transformation (FFT) with a Hanning window on 50 % overlapping blocks of 131,072 samples each and converted to sound pressure levels *re* 20 μPa. The resulting frequency resolution is only 0.39 Hz. Finally, 6 dB were subtracted to correct for the increased amplitude due to the summation of both time signals.

2.5. Flap Motion Measurements

The movement of the flexible flaps of a flap ring, positioned at mid-span, was measured using a high speed camera (Phantom V12.1-8 G-M, Vision Research) with a 35 mm Nikon lens, which was positioned below the test section (see Figure 6). The frame rate was set to 500 Hz with a total measurement duration of approximately 14 s. The exposure time per frame was 500 μs. Using the procedure described in [16], the time-series of the movement of the centroid point of each single flap of a chosen flap ring was derived from the camera recordings. These results were then converted to corresponding power spectral densities of the flap movement using a Burg algorithm [23].

Due to the fact that neighboring flaps were found to collide at high flow speeds as a consequence of the increased amplitude of the flap oscillations, the flap motion measurements were only performed up to Reynolds numbers of 26,000 to 28,500. For the case of the cylinder with six flaps, however, those measurements could only be conducted up to a Reynolds number of 20,900.

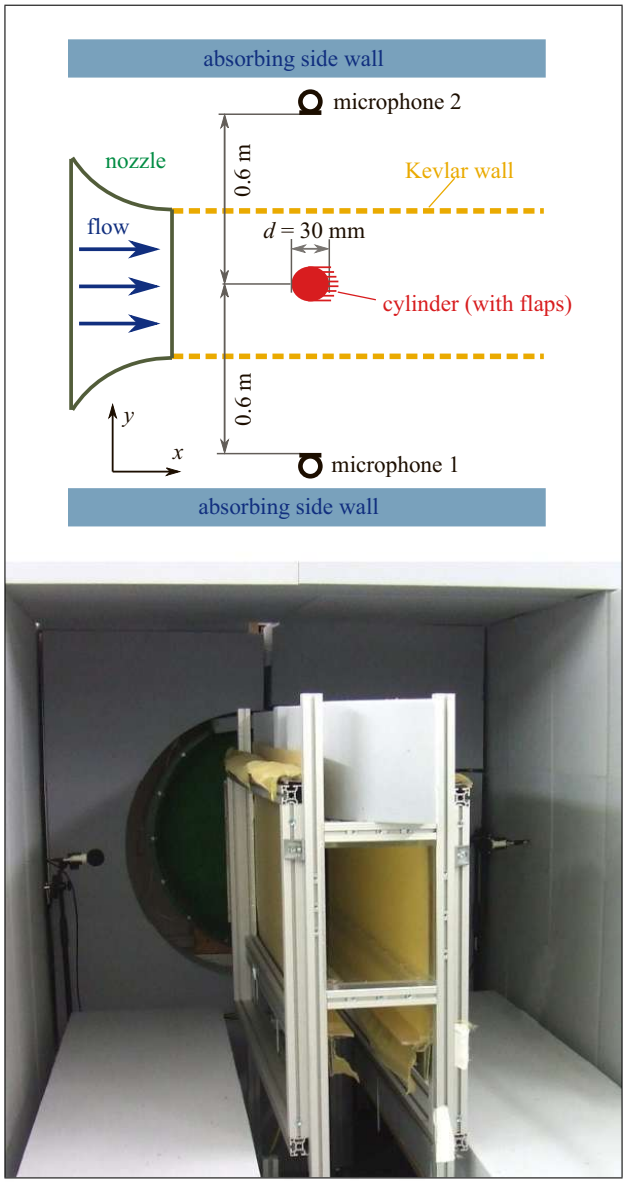

Figure 5. Setup used for the acoustic measurements. Top: Schematic (top view, not to scale), bottom: Photograph.

3. Results

3.1. Modal Analysis

The numerical modal analysis revealed that, for all cases where the flaps were not shortened (Figure 2a through 2d), the eigenmodes and eigenfrequencies in the examined range up to 250 Hz are identical. Furthermore, since the shape and material of each flap on the flap ring is identical, the eigenmodes are also the same for each flap.

The first eigenmode at 22 Hz corresponds to the first bending mode of the flap. The second mode (the first torsion mode) can be observed at a frequency of 39 Hz, while the third mode, which appears to be the second torsion mode, is visible at 97 Hz. Another bending mode, but in a direction perpendicular to the first bending mode at 22 Hz, occurs at 137 Hz. Due to the fact that the flaps are firmly attached to the cylinder body, the resulting shape of

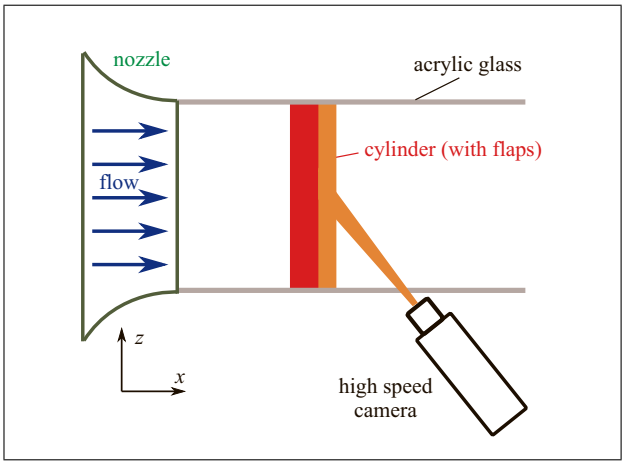

Figure 6. Schematic (side view) of the setup used for the flap motion measurements (not to scale)

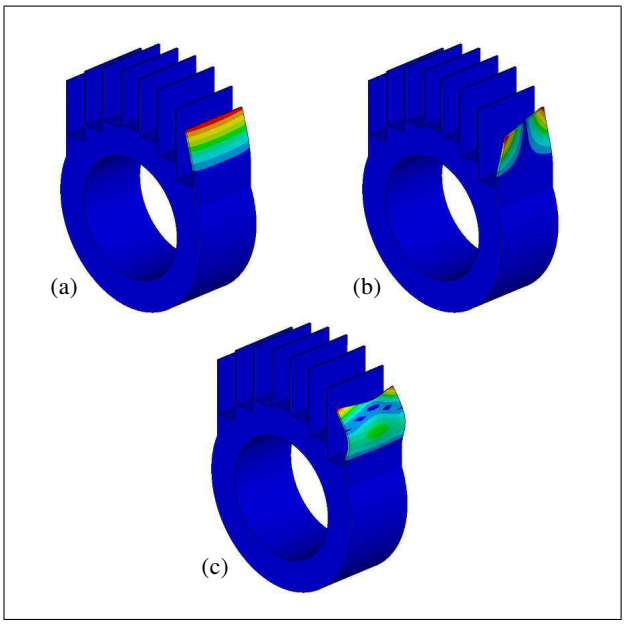

Figure 7. Three selected eigenmodes of the original flap ring with eight flaps. (a) 22 Hz (first bending mode), (b) 39 Hz (first torsion mode), (c) 137 Hz.

that particular mode resembles a cambered surface. Further eigenfrequencies of 156 Hz, 236 Hz and 243 Hz were found, the corresponding modes, however, take more complex shapes. Of course, it cannot be expected that each eigenmode will affect the vortex shedding cycle in the same way, it seems rather more likely that only those eigenmodes that lead to a strong deformation of the flap in the direction perpendicular to the shear layer will have an influence. As an example, Figure 7 shows the shapes of three selected eigenmodes of one flap from the original flap ring with eight flaps.

For the case where the remaining two outer flaps were shortened (see Figure 2e), the modal analysis revealed completely different eigenmodes and eigenfrequencies. For example, the frequency of the first bending mode increases to a value of 86 Hz, that of the first torsion mode to 107 Hz and that of the second torsion mode to 171 Hz. Table I lists the eigenfrequencies of the different flap rings.

When the thickness of the flaps is increased or decreased by 5 % compared to their nominal thickness of 0.3 mm, the modal analysis revealed that the corresponding eigenfrequencies increase/decrease by about 3 to 5 % as well. If the thickness increases/decreases by 10 %, the eigenfrequencies subsequently show an increase/decrease of about 8 to 10 %. This agrees with basic mechanical theory, where an increase of the thickness of a rectangular plate will result in an increase of the corresponding eigenfrequencies (see for example [24]).

3.2. Results from Acoustic Measurements

The sound pressure level spectra measured for the cylinders from Figure 2 as well as for the reference cylinder are shown in Figure 8 as a function of Strouhal number based on the outer diameter. In addition, the spectra obtained for the empty wind tunnel are included. It can be seen that in the region around the vortex shedding peak the signals obtained for the different cylinders exceed the background noise by more than 40 dB.

Basically, the above discussed effect that the vortex shedding peak obtained for the flap cylinders suddenly jumps towards a higher Strouhal number at Reynolds numbers between 23,300 and 26,000 is visible, while the peak of the reference cylinder stays at a constant value just above 0.2. Thereby, the spectra obtained for the cases with unshortened flaps all show essentially the same behavior, while the peak obtained for the cylinder with the two shortened flaps (Figure 2e) jumps to a noticeably lower Strouhal number. This implies that, in air, the observed jump is not caused by an oscillation of the flap system as a whole (consisting of eight equally-spaced flaps with a fluid volume in between), but essentially by the movement of the outer flaps. In contrast, in the water tunnel experiments in [15], the lock-in was found to occur between the vortex shedding and a traveling wave running through the bundle of flexible flaps in a direction perpendicular to the flow and the cylinder axis. This difference is presumably caused by the different properties of the two fluids. Due to the fact that the bulk modulus of water is much higher than that of air, the oscillating system consisting of the silicone flaps and the fluid-filled spaces between those flaps is much stiffer in water than in air, leading to a stronger coupling between the single flaps. Additionally, in the case of water the difference in density between flap and fluid is much smaller than in air.

To further illustrate the differences between the cases with the long flaps and the shortened flaps, Figure 9 shows the peak Strouhal number as a function of the Reynolds number based on cylinder diameter. Thereby, this peak Strouhal number represents the arithmetic mean of the peak Strouhal numbers from both measurements. While the resulting Strouhal number for the original cylinder with eight flaps suddenly jumps from values around 0.25 at $Re \leq 23{,}300$ to a value of about 0.3 at $Re = 26{,}000$, the Strouhal number for the cylinder with shortened flaps

Table I. Numerically obtained eigenfrequencies of the different flap rings shown in Figure 2.

Flap rings	Eigenfrequencies (Hz) 1st mode	2nd mode	3rd mode	4th mode	5th mode	6th mode	7th mode
8, 6, 4 and 2 flaps	22	39	97	137	156	236	243
2 flaps, shortened	86	107	171	–	–	289	–

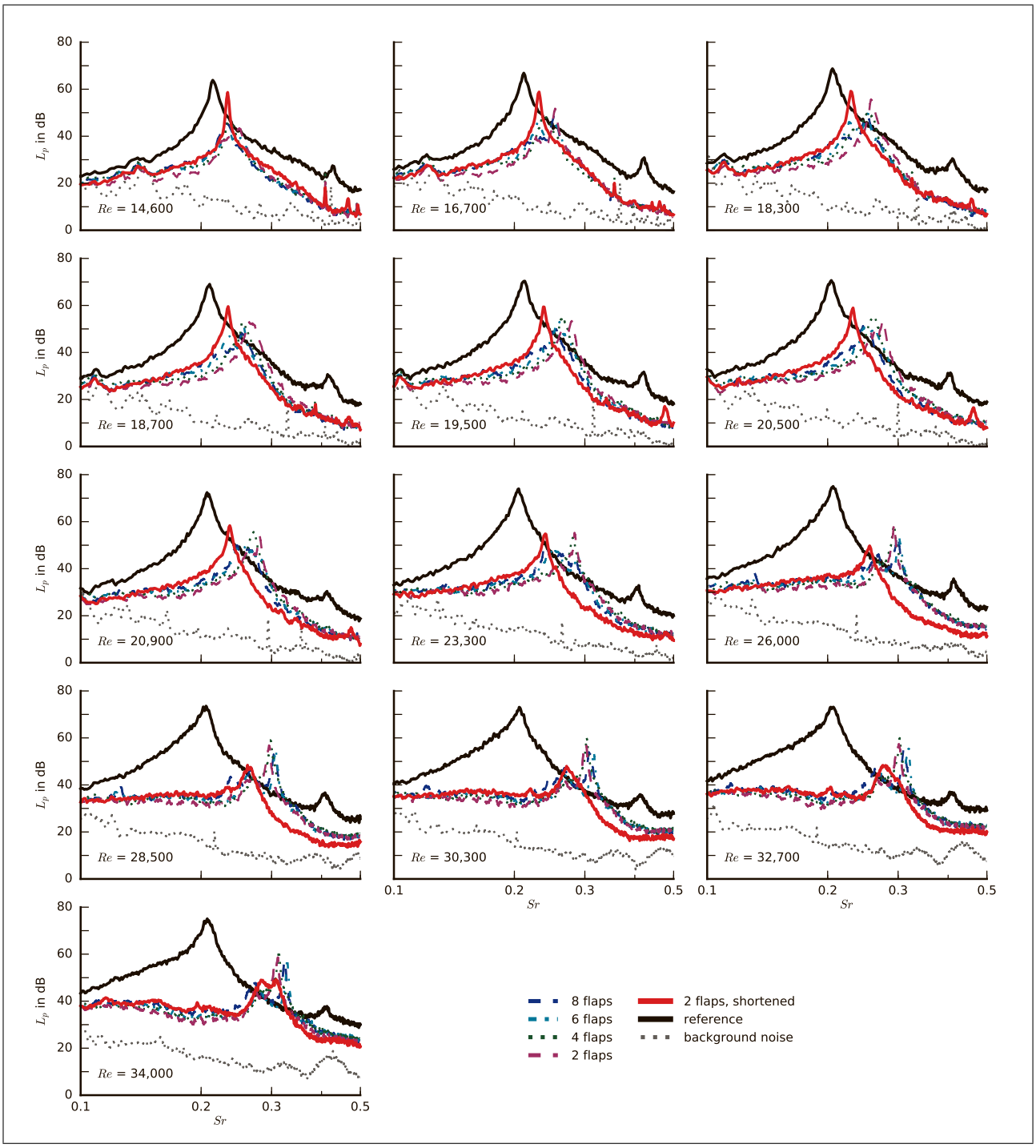

Figure 8. (Colour online) Measured sound pressure level spectra ($re\ 2{\cdot}10^{-5}$ Pa) around the vortex shedding peak.

changes from about 0.24 at Re = 23,300 to approximately 0.26 at Re = 26,000. For the reference cylinder, the Strouhal number takes values between 0.22 at the lowest Reynolds number and 0.21 at the highest Reynolds num-

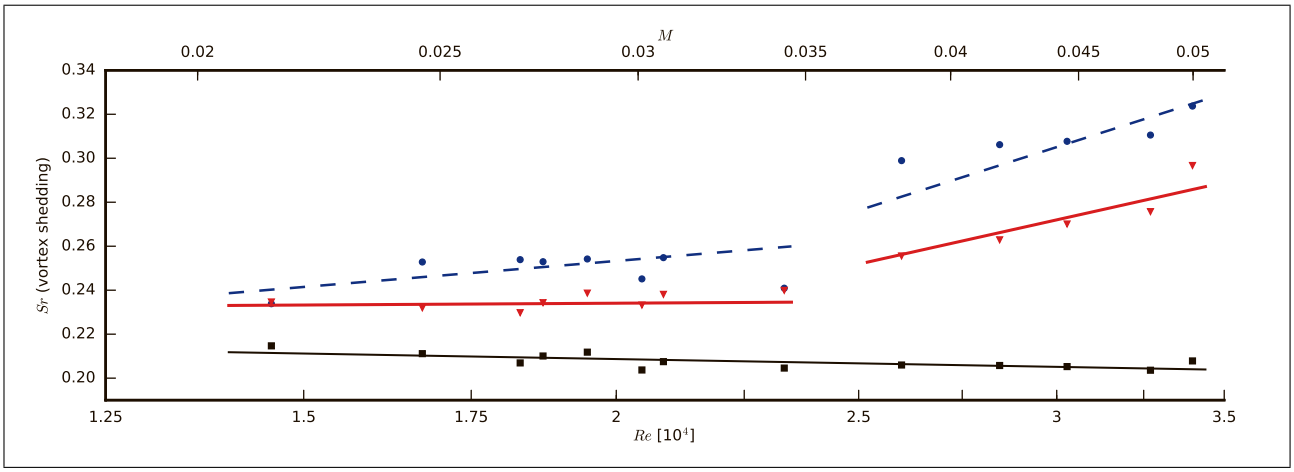

Figure 9. Dependence of the peak Strouhal number Sr obtained from the acoustic measurements on the Reynolds number Re based on cylinder diameter, the lines represent linear approximations of the measured data (■ baseline cylinder, ● 8 flaps, ▼ 2 flaps, shortened).

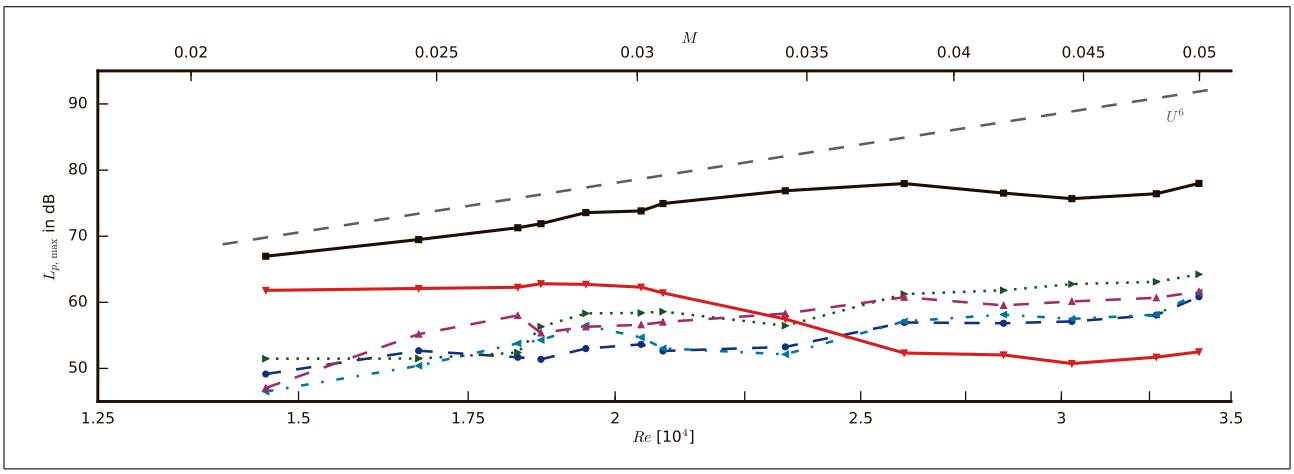

Figure 10. Dependence of the peak sound pressure level $L_{p,\max}$ obtained from the acoustic measurements on the Reynolds number Re based on cylinder diameter (■ baseline cylinder, ● 8 flaps, ◀ 6 flaps, ▶ 4 flaps, ▲ 2 flaps, ▼ 2 flaps, shortened. Dashed line: theoretic dipole).

ber, which is in good agreement with the theoretical value of 0.21 [25] known for this flow regime (the subcritical range, characterized by a laminar near-wake with vortex street instability).

In addition, Figure 10 shows how the maximum sound pressure level of the vortex shedding peak of the different cylinders changes with Reynolds number Re and Mach number M. For the baseline cylinder, the peak level increases with increasing Re. At Reynolds numbers up to approximately 26,000, the peak level follows the theoretical scaling of a dipole sound source with the sixth power of the flow speed. At higher Reynolds numbers, the peak level somewhat decreases, leading to a slightly reduced velocity dependence. This trend was also observed in [14] and can be attributed to the complex velocity dependence of cylinder flow noise in general and to a change in boundary layer thickness on the Kevlar windows of the test section, which results in a decrease in measured peak amplitude. It is clearly visible from Figure 10 that the presence of the flexible flaps leads to a strong reduction of the vortex shedding peak level. The cause of this noise reduction is assumed to be the fact that a part of the energy contained in the boundary layer is needed to move and deform the flaps, and hence less energy is converted to noise. This agrees with the work of Kunze and Brücker [15] who found that the flaps lead to a decrease of the rms-values of the velocity components within the wake region. Teksin and Yayla [19] also observed that the presence of a flexible splitter plate decreases the turbulent kinetic energy and the rms-values of the streamwise and transverse velocities of the flow field.

However, while the peak level of the cylinder models with long flaps show a similar increase with Reynolds number as the reference cylinder without flaps, the peak level obtained for the cylinder with the shortened flaps shows a different behavior. At Reynolds numbers up to 20,900, the level remains approximately constant at around 62 dB. With further increasing Reynolds number, the peak level decreases considerably. A comparison with Figure 8 reveals that the vortex shedding peaks appear much broader in this range, suggesting that the decrease in peak level does not correspond to a decrease in

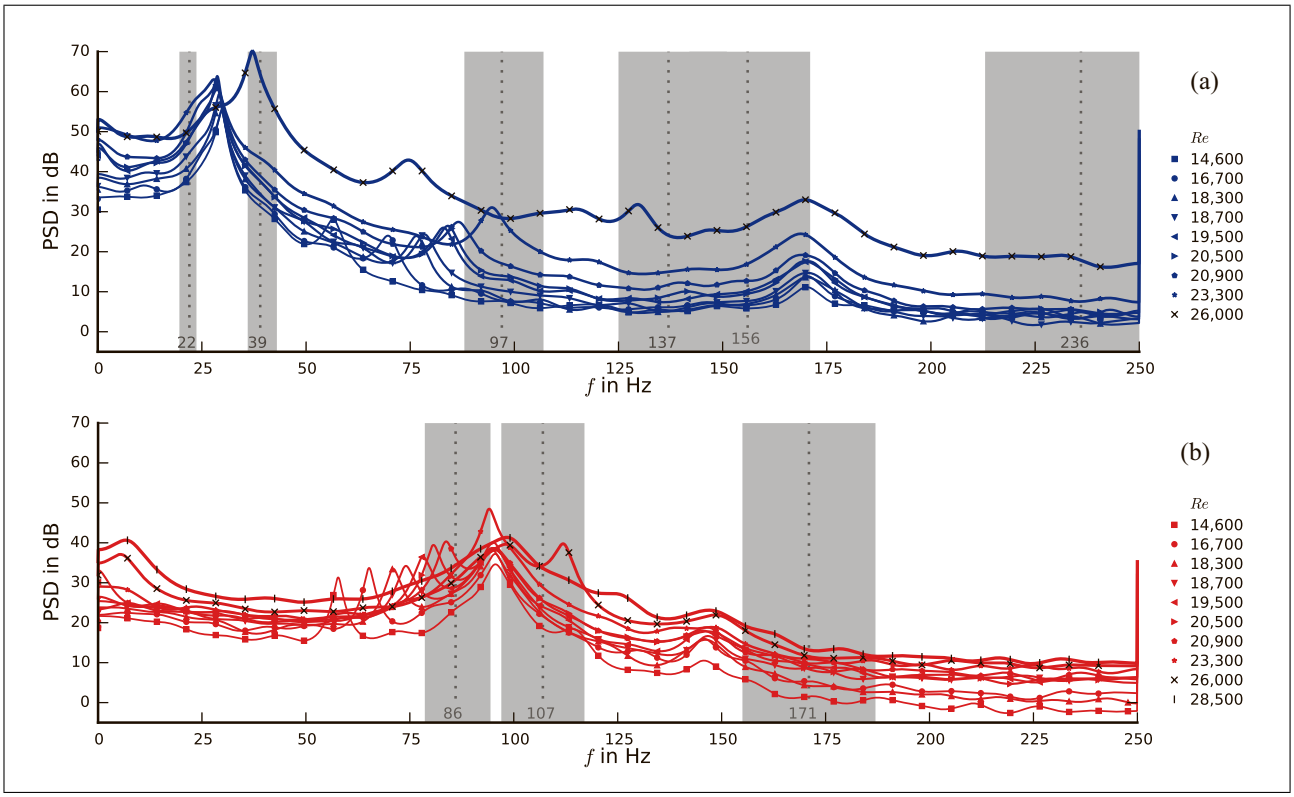

Figure 11. Spectra obtained from the flap motion measurements (vertical lines represent eigenfrequencies obtained numerically, gray bands correspond to deviations in eigenfrequency if a ±10 % variation of the flap thickness is assumed). (a) 8 flaps, (b) 2 flaps, shortened.

sound power or sound intensity of the peak, but mainly to a change of the spectral shape of the peak. Such a change is not visible in the spectra obtained for the other flap cylinders.

Since it was shown in [16] that the aeolian tones generated by the flap cylinder are strongly coupled to the movement of the flaps, the following section will provide results from the flap motion measurements.

3.3. Results from Flap Motion Measurements

Figure 11 shows spectra obtained from the flap motion measurements performed with the high-speed camera. As an example, spectra are shown for one outer flap of the original flap cylinder with eight flaps (Figure 2a) and that with the two shortened flaps (Figure 2e). Each figure additionally contains the theoretical eigenfrequencies derived from the modal analysis as given in Table I. Also included are the resulting eigenfrequency ranges derived numerically when a deviation of the flap thickness of ±10 % is assumed. The spectra obtained for the remaining cylinders were basically identical to those obtained for the cylinder with 8 flaps and thus are not shown here.

The spectra from the flap motion measurements reveal that the flaps do not only perform just one single motion related to the vortex shedding at the cylinder, but rather they do perform a multitude of different oscillating motions, most of which are linked to the eigenfrequencies of the flaps. In case of the cylinder with 8 flaps (Figure 11a), the first peak seems to be linked to the first bending mode at 22 Hz or the first torsion mode at 39 Hz. The second peak, at frequencies above 50 Hz, can be associated with vortex shedding, as its frequency increases with increasing Reynolds number. The third peak is at a constant frequency of approximately 170 Hz. When the differences between a CAD model and the actual flap cylinders are taken into account, this third peak may be related to the eigenmode observed at 156 Hz. Interestingly, at the highest Reynolds number of 26,000 the shape of the flap motion spectrum differs from that obtained at lower Reynolds numbers. Most notably, this includes a shift of the first and strongest spectral peak towards higher frequencies, but also a generally increased amplitude of the flap movement. The measurement at the highest Reynolds number of 26,000 belongs to a case where the Strouhal number obtained from the acoustic measurements jumped to a notably higher value of around 0.3. This corresponds to a frequency of about 131 Hz. Around this frequency, the flap motion spectrum shows a strong peak, which can be assumed to be related to the eigenmode of the flap rings at 137 Hz, as shown in Figure 7c. As described in Section 3.1, this eigenmode is related to a bending motion of the flaps, although in a direction perpendicular to the first bending mode at 22 Hz. The result is a flap that repeatedly cambers and straightens with a frequency of 137 Hz, a process that is very likely to interact with the adjacent flow and the regular vortex shedding. The same shift occurred in the spectra obtained for the cylinder with only

the two outer flaps left (not shown here). It can therefore be concluded that the jump in the *Re*-*Sr*-plot is caused by a lock-in of the vortex shedding cycle with an eigenmode of the outer flaps.

The spectra obtained for the cylinder with two shortened flaps (Figure 11b) show considerable differences. At low Reynolds numbers, the first discernible peak is the one related to the vortex shedding (at frequencies above 50 Hz). At the two highest Reynolds numbers of 26,000 and 28,500 (which is above the jump), this vortex shedding peak is already merged with another peak at a fixed frequency of about 95 Hz, which can be assumed to be related to the first bending mode of the short flaps at a frequency of 86 Hz. Thus, in case of the shortened flaps, the sudden shift of the Strouhal number is caused by a lock-in with the first bending mode of the flaps. A second, much smaller local maximum is visible in the flap motion spectra around 140 Hz. This peak does not seem to be related to any eigenfrequency of the flap ring, as the modal analysis predicted the next eigenmode at a frequency of 170 Hz. The cause of this small peak is currently not clear.

Overall, the present analysis of the flap motion reveals that the observed jump of the Strouhal number related to vortex shedding is caused by a lock-in with an eigenmode of the flaps. In case of the unshortened flaps, this eigenmode belongs to a bending motion of the flaps, but in a direction perpendicular to the first bending mode. For the case with the two shortened flaps, the lock-in happens with the frequency of the first bending mode. It appears, however, that the lock-in always happens with the next "available" mode, and hence the mode with an eigenfrequency just above the natural vortex shedding frequency. It is not fully clear whether the exact shape of this mode is important, as in the present case the corresponding modes were two different bending modes. Basically, this behavior indicates that such effects may also occur at even higher frequencies, when the vortex shedding cycle locks-in with the next higher eigenfrequency. It was not possible to test this hypothesis with the present setup, since with further increasing flow speed neighboring flaps started to collide, rendering the analysis of the flap motion impossible.

4. Conclusions

In a recent wind tunnel study on the vortex shedding noise generated by a cylinder equipped with eight flexible flaps made of silicone rubber it was found that the flaps alter the frequency of the vortex shedding. This led to a sudden jump in the corresponding plot of Strouhal number versus Reynolds number. The aim of the present study is to further investigate the effect of the flexible flaps on the vortex shedding and the possible cause of the Strouhal number jump. To this end, the original cylinder with eight flaps was modified by subsequently cutting off flaps, until only the two outermost flaps remained. This was done in order to verify whether all flaps contribute to the Strouhal number jump or if only the outer flaps are necessary. Finally, the remaining outer flaps were additionally shortened in order to investigate the effect of the flap size on the Strouhal number. For each resulting cylinder model, acoustic measurements were performed in an aeroacoustic wind tunnel at low Reynolds numbers, using two microphones on opposite sides of the wind tunnel test section. A high speed camera was used to capture the motion of the flaps of one flap ring approximately at mid span. In addition to the wind tunnel experiments, a modal analysis of the different configurations was performed numerically.

The measurement results revealed that the spectra of the cylinders with flaps of equal length show essentially the same behavior, meaning the Strouhal number jumps to the same value within the same Reynolds number range between 23,300 and 26,000. This leads to the conclusion that the observed lock-in effect between the vortex shedding cycle and the flap motion does not seem to be caused by an oscillation of a whole system of flaps, but rather by the movement of the two outer flaps.

Additionally, the analysis of the flap motion spectra and a subsequent comparison with the eigenmodes of the single flaps showed that the observed Strouhal number jump is caused by a lock-in of the natural vortex shedding cycle with the next higher flap eigenfrequency. This means that flexible flaps (which can basically be understood as a flat plate of which one side is clamped and three sides are free) could be specifically designed in order to obtain desired eigenfrequencies, thus controlling the Strouhal number associated with vortex shedding.

Acknowledgments

This work was partly funded within the framework of PEL-SKIN project EU- FP7, GA no. 334954. The position of Professor Christoph Brücker is co- funded by the BAE Systems Sir Richard Olver Chair and the Royal Academy of Engineering Research Chair, which is gratefully acknowledged.

References

[1] B. Etkin, G. K. Korbacher, R. T. Keefe: Acoustic radiation from a stationary cylinder in a fluid stream (Aeolian tones). Journal of the Acoustical Society of America **29** (1957) 30–36.

[2] R. D. Blevins: Review of sound induced by vortex shedding from cylinders. Journal of Sound and Vibration **92** (1984) 455–470.

[3] V. Strouhal: Über eine besondere Art der Tonerregung. Annalen der Physik **241** (1878) 216–251.

[4] M. M. Zdravkovich: Review and classification of various aerodynamic and hydrodynamic means for suppressing vortex shedding. Journal of Wind Engineering and Industrial Aerodynamics **7** (1981) 145–189.

[5] K. Kiyoung, H. Choi: Control of laminar vortex shedding behind a circular cylinder using splitter plates. Physics of Fluids **8** (1996) 479–486.

[6] H. Akilli, B. Sahin, N. F. Tumen: Suppression of vortex shedding of circular cylinder in shallow water by a splitter plate. Flow Measurement and Instrumentation **16** (2005) 211–219.

[7] A. Roshko: On the wake and drag of bluff bodies. Journal of the Aeronautical Sciences (2012) 124–132.

[8] H. C. Lim, S. J. Lee: Flow control of a circular cylinder with O-rings. Fluid Dynamics Research **35** (2004) 107–122.

[9] N. W. M. Ko, Y. C. Leung, J. J. J. Chen: Flow past V-groove circular cylinders. AIAA Journal **25** (1987) 806–811.

[10] T. Igarashi: Effect of tripping wires on the flow around a circular cylinder normal to an airstream. Bulletin of JSME **29** (1986) 2917–2924.

[11] S. J. Lee, H. C. Lim, M. Han, S. S. Lee: Flow control of circular cylinder with a V-grooved micro-riblet film. Fluid Dynamics Research **37** (2005) 246–266.

[12] P. W. Bearman, J. K. Harvey: Control of circular cylinder flow by the use of dimples. AIAA Journal **31** (1993) 1753–1756.

[13] B. Levy, Y. Liu: The effects of cactus inspired spines on the aerodynamics of a cylinder. Journal of Fluids and Structures **39** (2013) 335–346.

[14] T. F. Geyer, E. Sarradj: Circular Cylinders with Soft Porous Cover for Flow Noise Reduction. Experiments in Fluids **57** (2016) 1–16.

[15] S. Kunze, C. Brücker: Control of Vortex Shedding on a Circular Cylinder Using Self-Adaptive Hairy-Flaps. Comptes Rendus Mécanique **340** (2012) 41–56.

[16] L. Kamps, T. F. Geyer, E. Sarradj, C. Brücker: Vortex shedding noise of a cylinder with hairy flaps. Journal of Sound and Vibration **388** (2017) 69–84.

[17] G. Grimminger: The effect of rigid guide vanes on the vibration and drag of a towed circular cylinder. Report No. DTMB-504, David Taylor Model Basin, Washington DC, 1945.

[18] S. Shukla, R. N. Govardhan, J. H. Arakeri: Dynamics of a flexible splitter plate in the wake of a circular cylinder. Journal of Fluids and Structures **41** (2013) 127–134.

[19] S. Teksin, S. Yayla: Effects of Flexible Splitter Plate in the Wake of a Cylindrical Body. Journal of Applied Fluid Mechanics **9** (2016).

[20] E. Sarradj, C. Fritzsche, T. F. Geyer, J. Giesler: Acoustic and aerodynamic design and characterization of a small-scale aeroacoustic wind tunnel. Appl Acoust **70** (2009) 1073–1080.

[21] J. B. Barlow, W. H. Rae, A. Pope: Low-speed wind tunnel testing. Third edition, John Wiley & Sons, 1999.

[22] P. D. Welch: The use of fast Fourier transform for the estimation of power spectra: a method based on time averaging over short, modified periodograms. IEEE Trans. Audio and Electroacoustics **15** (1967) 70–73.

[23] P. Stoica, R. Moses: Introduction to Spectral Analysis. Prentice-Hall, Upper Saddle River, NJ, 1997.

[24] F. J. Fahy: Foundations of engineering acoustics. Elsevier Academic Press, London, 2000.

[25] H. Schlichting, K. Gersten: Boundary-layer theory. Springer Verlag, Berlin Heidelberg, 9th edition, 1997.